Journal of Molecular Modeling (2018) 24:324
https://doi.org/10.1007/s00894-018-3866-6

ORIGINAL PAPER

^{13}C-^{1}H coupling constants as a conformational tool for structural assignment of quinic and octulosonic acid

Rabia Hameed[1,2] · Tanja van Mourik[2] · Afsar Khan[1]

Received: 6 July 2018 / Accepted: 5 October 2018

Abstract

A complete set of NMR coupling constants ($^{1}J_{C\text{-}H}$, $^{2}J_{C\text{-}H}$, $^{3}J_{C\text{-}H}$, and $^{3}J_{H\text{-}H}$) were calculated for the eight stereoisomers of quinic acid, at the B3LYP/6-311G(d,p)/PCM(methanol) level of theory. The Fermi contact term of the coupling constants was computed with a modified, uncontracted, version of the 6-311G(d,p) basis set, with additional tight polarization functions. ^{1}H and ^{13}C NMR chemical shifts were determined at the same level using the gauge-invariant atomic orbital (GIAO) method. The magnitude of the spin-spin coupling constants was found to be affected by the orientation (axial or equatorial) of the coupling proton and the orientation of the hydroxy group on the coupling carbon, whereas the chemical shifts depend on the presence or absence of electron-withdrawing hydroxy groups attached to the carbon atoms involved.

Keywords ^{13}C-^{1}H coupling constant · Quinic acid · Stereoisomers · Octulosonic acid · Relative stabilities · Density functional theory

Introduction

Quinic acid (1,3,4,5-tetrahydroxycyclohexanecarboxylic acid) is a widely occurring natural secondary metabolite, considered as a chiron store for the synthesis of a number of natural products [1, 2]. Quinic acid has eight different stereoisomers, which differ in the stereochemistry of the chiral carbon atoms (C1, C3, C4, and C5) of the cyclohexane moiety (see Fig. 1). Among these stereoisomers, there are two pairs of enantiomers and four meso (i.e., optically inactive) forms. The pairs of enantiomers are (−)- and (+)-quinic acid and (−)- and (+)-*epi*-quinic acid, whereas the meso forms include *cis*-, *muco*-, *neo*- and *scyllo*-quinic acid. All these isomers can be derived from (−)-quinic acid by inversion at one or two stereogenic centers: inversion at C1 gives (−)-*epi*-quinic acid; inversion at C3 yields *muco*-quinic acid; inversion at C5 gives *cis*-quinic acid; inversion at both C3 and C4 gives *neo*-quinic acid, and inversion at C4 and C5 yields *scyllo*-quinic acid [3]. Among these possible stereoisomers, (−)-quinic acid is readily found in a variety of diverse natural products [4]. Isolation of quinic acid from plants by chromatographic techniques dates back to the 1950s; in 1953, it was isolated as pure *l*-quinic acid through column chromatography on anion exchange resin [5]. In 1989, four different tetragalloyl quinic acids were isolated from commercial tannic acid. These were identified as a new class of human immunodeficiency virus (HIV) reverse transcriptase inhibitors [6]. Dicaffeoyl and tetragalloyl derivatives of quinic acid possess great potential to combat various diseases. Its caffeoyl derivatives [7] are reported as therapeutic agents having cytotoxic, antioxidant [8, 9], anti-Alzheimer, hepatoprotective [10], hepatotoxic [11], neuroprotective, and neurotrophic effects [12].

All eight quinic acid stereoisomers occur in two different chair conformations, which can be converted into each other by a "chair flip" [13]. These two chair conformations have opposite axial/equatorial positions of the carbonyl and hydroxyl groups. The prevalent conformer may vary depending on factors such as the particular environment. For example, Scholz–Böttcher et al. recorded NMR data on different quinic

Electronic supplementary material The online version of this article (https://doi.org/10.1007/s00894-018-3866-6) contains supplementary material, which is available to authorized users.

✉ Tanja van Mourik
tanja.vanmourik@st-andrews.ac.uk

✉ Afsar Khan
afsarhej@gmail.com

[1] Department of Chemistry, COMSATS University Islamabad, Abbottabad Campus, Islamabad 22060, Pakistan

[2] School of Chemistry, University of St Andrews, North Haugh, St Andrews KY16 9ST, UK

Published online: 26 October 2018

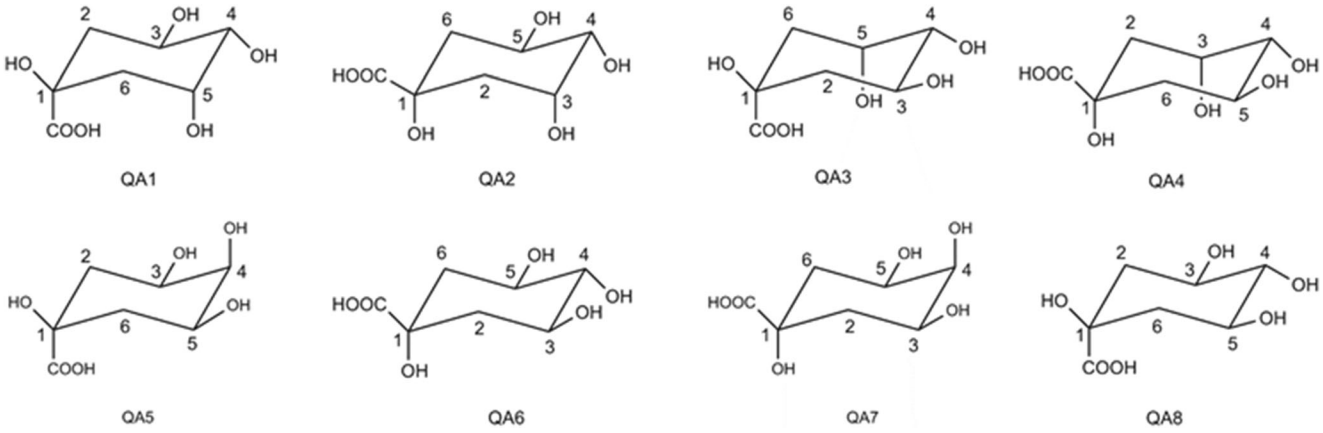

Fig. 1 Stereoisomers of quinic acid: QA1 = (−)-*epi*-quinic acid; QA2 = (−)-quinic acid; QA3 = (+)-*epi*-quinic acid; QA4 = (+)-quinic acid; QA5 = *cis*-quinic acid; QA6 = *muco*-quinic acid; QA7 = *neo*-quinic acid; QA8 = *scyllo*-quinic acid

acid stereoisomers, including the ammonium salt of *epi*-quinic acid [14]. They concluded that the two possible chair conformations for this stereoisomer are in equilibrium, with a preference for the stereoisomer that has the carboxyl group in the axial position.

Nucleid magnetic resonance (NMR) has been one of the most popular experimental techniques to study quinic acid derivatives. In 1970, Corse and Lundin reported an experimental NMR study on (+)- (−) and (±) *epi*-quinides as well as *scyllo*-quinic acid [15]. The NMR spectrum of *scyllo*-quinic acid indicated that all three hydroxy groups are in the equatorial position. *Neo*-quinic acid was reported for the first time by Scholz–Böttcher et al. in 1991 [14]. They studied a mixture of six stereoisomeric quinic acids, four γ-quinides, and three δ-quinides. In addition to *neo*-quinic acid, two *meso*-quinic acids and several quinides were also reported for the first time [14]. Pauli et al. studied naturally occurring hydroxycinnamoylquinic acids using NMR [4]. A full set of chemical shift values and spin-spin coupling constants were obtained. Specific rules for proton substituent chemical shifts were obtained, which allowed to distinguishing between different position isomers and single caffeoyl units in substituted quinic acids. Other experimental techniques have been employed as well. Deshpande et al. synthesized four quinic acid isomers, namely *epi*-, *muco*-, *cis*-, and *scyllo*-quinic acid, to develop a tandem liquid chromatography-mass spectrometry (LC-MS) method to identify several quinic acid stereoisomers [3]. They reported that the stereoisomers can be chromatographically resolved and identified by their behavior in tandem MS spectra.

Computational studies have been shown to be an invaluable tool in differentiating the conformers of natural products. For example, Härtner and Reinscheid studied the diastereomers of menthol using experimental NMR and DFT calculations [16]. Differences in the ^{13}C chemical shifts allowed the differentiation of the prochiral methyl groups of the isopropyl substituent of menthol. In the present investigation, proton and carbon NMR spectroscopic properties are calculated to aid structural assignment of natural quinic acid and its stereoisomers. Although the literature provides a number of reports of quinic acid characterized on the basis of NMR spectroscopic techniques, there are no unambiguous data available to elucidate the structures of the eight possible stereoisomers of quinic acid. Furthermore, the stereochemistry of the stereo centers cannot be deduced from proton and carbon NMR chemical shifts only. However, the ^{1}H-^{1}H coupling constant values of the axial and equatorial protons may vary enough with the axial and equatorial arrangement of the COOH and OH groups to elucidate the correct structure of the compounds. The aim of the current study is to find correlations between the computed NMR data and the structure of the stereoisomers, such as the orientation (equatorial or axial) of the substituents. These correlations can then be used to provide assignments of the positions of the hydroxy groups for quinic acids and related compounds (such as octulosonic acid) based on NMR data.

Methods

All calculations were performed using Gaussian 09 [17]. Geometries were fully optimized with the B3LYP [18–20] density functional and the 6-311G(d,p) [21] basis set. Solvent effects were included using the polarizable continuum model (PCM) [22] using the integral equation formalism (IEFPCM [23]) variant and methanol as the solvent. As mentioned above, each stereoisomer has two separate chair conformations, with the COOH group either axial or equatorial [13]. We have chosen the conformers following Ref. [14], i.e., COOH equatorial for quinic acid, *muco*-quinic acid, and *neo*-quinic acid and axial for the other stereoisomers. To optimize hydrogen bonding, the OH-groups attached to carbons 1, 3, 4, and 5 (see Fig. 1 for atom labeling) were oriented such as to form a chain of hydrogen bonds. This can be achieved in two directions, which we label (arbitrarily) clockwise and anti-

clockwise. Cartesian coordinates of the optimized structures can be found in the Supporting Information (Table S5). For each quinic acid stereoisomer, we chose the one (clockwise or anti-clockwise) with the lowest energy.

^{1}H- and ^{13}C-NMR shielding tensors and proton–proton and carbon–proton spin-spin coupling constants were subsequently calculated at the same level of theory. For compound 1, the calculations used DMSO (dimethyl sulfoxide) as the implicit solvent, to match the experimental conditions [24]. For (−)-quinic acid and compounds **1** and **2** (see below) the spin-spin couplings were also calculated with B3LYP/EPR-II in implicit solvent. The EPR-II basis set is a double zeta basis set with polarization functions and an enhanced s-part and is optimized for the calculation of hyperfine coupling constants [25]. The shielding tensors were computed using the gauge-invariant atomic orbital (GIAO) method [26–28]. Chemical shifts were calculated by subtracting the ^{1}H and ^{13}C chemical shieldings from the corresponding shielding of TMS (tetramethylsilane), calculated at the same level of theory. Proton–proton and carbon–proton spin-spin coupling constants ($^{2}J_{H\text{-}H}$, $^{3}J_{H\text{-}H}$, $^{4}J_{H\text{-}H}$, $^{1}J_{C\text{-}H}$, $^{2}J_{C\text{-}H}$ and $^{3}J_{C\text{-}H}$) were calculated as the sum of the four Ramsay terms [29] (i.e., Fermi contact, spin dipolar, diamagnetic spin-orbit, and paramagnetic spin-orbit terms). The calculation of the spin-spin coupling constants employed the "mixed" keyword, which calculates the spin-spin couplings in a two-step process: in the first step, the user-specified basis set is modified for the calculation of the Fermi contact term by uncontracting the basis set and adding tight polarization functions; in the second step the other terms are calculated with the unmodified basis set.

Results and discussion

Relative stabilities of the quinic acid stereoisomers

Figure 1 shows the eight possible stereoisomers of quinic acid, labeled QA1 to QA8. The carbon atoms are numbered starting from the carbon that carries the COOH group. Note that this is the same numbering as that used by Abrankó and Clifford [13].

Figure 2 shows the optimized structures of the quinic acid isomers. Their relative energies are shown in Table 1. Note that each of the (+) / (−) quinic acid and (+) / (−) *epi*-quinic acid enantiomers are mirror images and therefore have the same energy. The most stable isomer was found to be (+) / (−) quinic acid. The *neo*-quinic acid isomer is the next most stable isomer, with an energy 4.82 kcal/mol relative to the global minimum. The relative stabilities of the remaining isomers are around 6 kcal/mol. Thus, according to DFT, the order of stability of the quinic acid stereoisomers is (−)-quinic acid = (+)-quinic acid > *neo*-quinic acid > *cis*-quinic acid ≈ *muco*-quinic acid ≈ (+)-*epi*-quinic acid = (−)-*epi*-quinic acid ≈ *scyllo*-quinic acid.

Validation of level of theory

Although mass spectra and ^{1}H and ^{13}C chemical shifts of the quinic acid compounds are available in the literature [3], the mass spectra of the different isomers often give very similar peaks and fragmentation patterns, complicating distinguishing between different stereoisomers. In the LC-MS study of Deshpande et al. [3], not all stereoisomers of quinic acid could be distinguished based on their mass spectra. This is a common finding for isomeric compounds. It is therefore important to determine the coupling constants.

To validate the chosen level of theory, we compare calculated and experimental couplings, where experimental data are available (i.e., for (−)-quinic acid [4] and for two other compounds, see below). A comparison of the experimental and theoretical J_{HH} couplings for (−)-quinic acid is shown in Table 2. Note that C2 and C6 have two hydrogens attached to them, one of which is in the axial, and the other in the equatorial position. In (−)-quinic acid, the hydrogen attached to C3 is in the equatorial position, whereas the hydrogens attached to C4 and C5 are in the axial position. Table 2 shows that the calculated couplings are in good agreement with the experimental ones (largest deviation: 2.3 Hz with the EPR-II (mixed) basis set).

To verify the accuracy of the calculations for ^{13}C-^{1}H coupling constants, the same methods were applied to two other compounds for which experimental structural and NMR data are available: an octulosonic acid derivative (**1**), which is a phenolic compound found in the roots of yacon (*Smallanthus sonchifolius*), a perennial daisy grown in the Andes, and a phenylpropanoyl 2,7-anhydro-3-deoxy-2-octulosonic acid derivative (**2**) isolated from horseweed (*Conyza canadensis*), an annual plant native to Central and North America. The structure of compound **1**, 1*R*,2*S*,3*R*,4*R*,5*S*,7*R*)-4-hydroxy-7-hydroxymethyl-2,3-bis[3-(3,4-dihydroxyphenyl)-1-oxo-2-propenyloxy]-6,8-dioxabicyclo[3.2.1]octan-5-carboxylic acid, was established on the basis of mass spectrometry, NMR spectra, and circular dichroism analysis [30]. Three-bond ($^{3}J_{CH}$) ^{13}C-^{1}H spin-couplings were used to determine the relative configurations at C1, C2, C3, and C7 in compound **2**, *rel*-(1*S*,2*R*,3*R*,5*S*,7*R*)-methyl 7-caffeoyloxymethyl-2-hydroxy-3-feruloyloxy-6,8-dioxabicyclo[3.2.1]octane-5-carboxylate [24]. Compounds **1** and **2** are shown in Fig. 3.

Table 3 lists the experimental and computed coupling constants for compounds **1** and **2**. The computed ^{13}C-^{1}H couplings show good agreement with the experimental data. The largest deviation (1.92 Hz) again occurs for the EPR-II basis set; otherwise the two basis sets perform very similarly.

Tables S1–S3 in the Supporting Information show a comparison of the computed and experimental J_{HH} couplings of

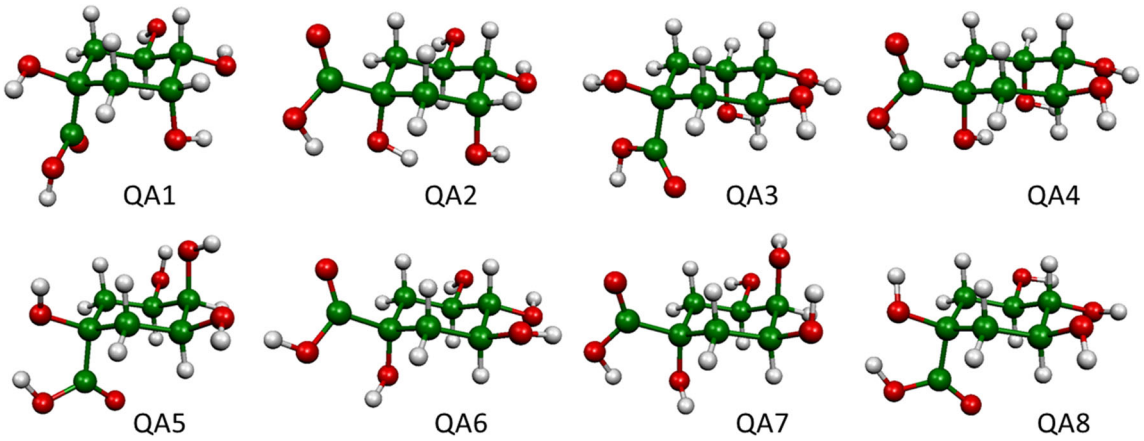

Fig. 2 Optimized geometries of stereoisomers QA1 – QA8

(−)-quinic acid and $^{3}J_{CH}$ couplings of compounds **1** and **2**. Linear regression shows good correlation between the experimental and computed results for (−)-quinic acid (R^2 values of 0.99 for both 6-311G(d,p) and EPR-II). The MAE (mean absolute error) and RMSE (root-mean-square error) values are 0.95/1.06 for 6-311G(d,p) and 0.86/1.12 for EPR-II, respectively. A similar good correlation is found for compound **1** (R^2 values of 0.99 for both basis sets), with MAE/RMSE values of 0.35/0.37 and 0.35/0.41 for 6-311G(d,p) and EPR-II, respectively. However, there is no meaningful correlation between the experimental and computed couplings for compound **2** (R^2 values of 0.28 and 0.30 for 6-311G(d,p) and EPR-II, respectively). This is likely due to different conformations of the side-groups in the experiment and calculation. The largest deviations (> 1 Hz) occur for $^{3}J_{C5\text{-}H3}$, $^{3}J_{C7\text{-}H2}$, and $^{3}J_{C3\text{-}H1}$, all involving carbon atoms with large, flexible substituents (carboxylic acid, feruloyl, and caffeoyl groups). Note that the absolute configuration of **2** was not determined [24].

Overall, B3LYP with either basis set gives good results for the ^{1}H-^{1}H coupling constants of (−)-quinic acid and ^{13}C-^{1}H coupling constants of compound 1. In the following discussion, we only report the 6-311G(d,p) (mixed) results.

Spin-spin coupling constants for the quinic acid stereoisomers

^{1}H-^{1}H couplings were computed for all optimized quinic acid isomers. The results are listed in Table 4. A full breakdown of the coupling constants into the four Ramsay terms is provided in the Supporting Information (Table S1). Note that the position (axial or equatorial) of the hydrogens attached to C3, C4 and C5 depends on the actual conformer (see Fig. 1). We have indicated in Table 4 whether the coupling is between two equatorial (eq-eq) or two axial (ax-ax) protons or between one axial and one equatorial (ax-eq) proton. Note that the couplings for the QA1/QA3 and QA2/QA4 pairs are equivalent.

For all couplings, the Fermi contact term is dominant (Table S1, Supporting Information). The two-bond $J_{H6ax\text{-}H6eq}$ and $J_{H2ax\text{-}H2eq}$ couplings are large in all isomers. Their magnitudes range from −12.9 to −16.3 Hz. In contrast, the magnitude of the four-bond $J_{H6eq\text{-}H2eq}$ coupling is small in all isomers (values below 3 Hz). Variation in the magnitude of the three-bond couplings can be related to the positions of the coupling protons. In general, $J_{ax\text{-}ax} >> J_{ax\text{-}eq} > J_{eq\text{-}eq}$. For example, the ax-ax couplings are around 9 Hz for $^{3}J_{H5\text{-}H4}$ and $^{3}J_{H4\text{-}H3}$ and around 11–12 Hz for $^{3}J_{H6ax\text{-}H5}$ and $^{3}J_{H3\text{-}H2ax}$. The $^{3}J_{ax\text{-}eq}$ values are smaller than the ax-ax couplings, but on average slightly larger (range of 3.1–6.0 Hz) than the $^{3}J_{eq\text{-}eq}$

Table 1 Relative energies (Relative to the most stable enantiomer pair QA2/4) (in kcal/mol) of the quinic acid isomers

Isomer		ΔE
QA1/3	(−)/(+) *epi*-quinic acid	6.17
QA2/4	(−)/(+) quinic acid	0.00
QA5	*cis*-quinic acid	6.13
QA6	*muco*-quinic acid	6.13
QA7	*neo*-quinic acid	4.82
QA8	*scyllo*-quinic acid	6.21

Table 2 Comparison of experimental and theoretical ^{1}H-^{1}H coupling constants (in Hz), computed with B3LYP for (−)-quinic acid

Coupling	Experimental[a]	6-311G(d,p) mixed	EPR-II mixed
$^{2}J_{H2ax\text{-}H2eq}$	14.5	− 16.3	− 16.8
$^{2}J_{H6ax\text{-}H6eq}$	13.2	− 14.6	− 14.4
$^{3}J_{H2eq\text{-}H3eq}$	3.7	3.2	3.9
$^{3}J_{H2ax\text{-}H3eq}$	3.3	4.1	3.3
$^{3}J_{H3eq\text{-}H4ax}$	3.2	4.2	3.9
$^{3}J_{H4ax\text{-}H5ax}$	9.2	9.3	9.1
$^{3}J_{H5ax\text{-}H6ax}$	11.0	12.1	12.6
$^{3}J_{H5ax\text{-}H6eq}$	4.7	5.5	5.8
$^{4}J_{H2eq\text{-}H6eq}$	2.0	3.1	2.6

[a] From Ref. [4]

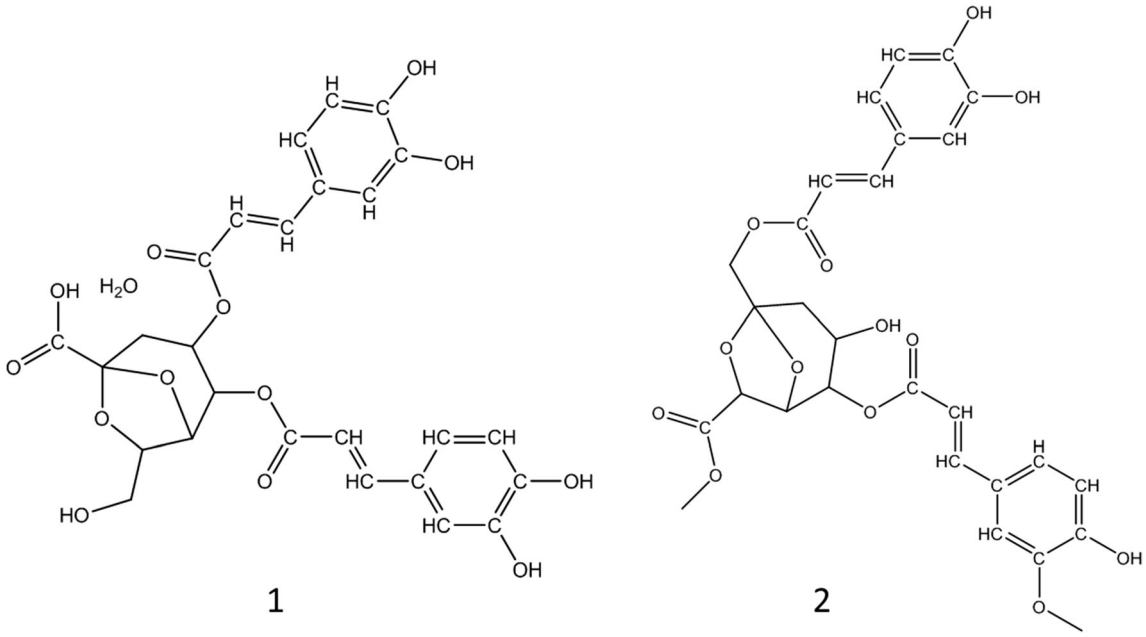

Fig. 3 Compounds **1** and **2**

values (3.8–3.9 Hz), though there is overlap in the magnitude of their values.

The one-, two-, and three-bond ^{13}C-^{1}H coupling constants are shown in Tables 5, 6, and 7, respectively. A full breakdown of the couplings into the four Ramsay terms is provided in the Supporting Information (Tables S2, S3, and S4, respectively). Like for the ^{1}H-^{1}H couplings, the ^{13}C-^{1}H couplings are largely dominated by the Fermi contact term.

In general, only very weak correlations were found between the couplings and corresponding geometrical parameters ($^{1}J_{CH}$: distance between the coupling atoms; $^{2}J_{CH}$: angle involving the coupling atoms and the bridging atom; $^{3}J_{CH}$: torsion involving the coupling atoms and the two bridging atoms in between; these geometrical parameters are also included in Tables S2, S3, and S4). Instead, we found that the couplings are primarily dependent on the orientation

Table 3 Comparison of experimental and theoretical ^{13}C-^{1}H coupling constants (in Hz), computed with B3LYP for compounds **1** and **2**

Coupling	Experimental[a]	6-311G(d,p) mixed	EPR-II mixed
Compound **1**			
$^{3}J_{C5\text{-}H7}$	5.8	6.17	5.52
$^{3}J_{C7\text{-}H5}$	5.9	6.46	5.84
$^{3}J_{C6\text{-}H4}$	5.4	5.59	5.03
$^{3}J_{C4\text{-}H6}$	5.4	5.84	5.19
$^{3}J_{C5\text{-}H3}$	4.1	3.85	3.46
$^{3}J_{C2\text{-}H4}$	3.8	3.54	3.24
Compound **2**			
$^{3}J_{C2\text{-}H7}$	5.6	5.94	5.90
$^{3}J_{C7\text{-}H2}$	4.9	6.34	6.36
$^{3}J_{C1\text{-}H3}$	5.1	5.87	5.87
$^{3}J_{C3\text{-}H1}$	5.0	6.24	6.19
$^{3}J_{C5\text{-}H3}$	5.0	6.87	6.92

[a] From Ref. [30] (compound **1**) and [24] (compound **2**)

Table 4 ^{1}H-^{1}H spin-spin coupling constants (in Hz) for all quinic acid isomers

Coupling	QA1/QA3	QA2/QA4	QA5
$^{2}J_{H6ax\text{-}H6eq}$	− 15.1 (ax-eq)	− 14.1 (ax-eq)	− 12.9 (ax-eq)
$^{2}J_{H2ax\text{-}H2eq}$	− 13.3 (ax-eq)	− 16.3 (ax-eq)	− 13.8 (ax-eq)
$^{3}J_{H6ax\text{-}H5}$	3.1 (ax-eq)	11.9 (ax-ax)	11.2 (ax-ax)
$^{3}J_{H6eq\text{-}H5}$	3.9 (eq-eq)	5.6 (ax-eq)	5.6 (ax-eq)
$^{3}J_{H5\text{-}H4}$	3.7 (ax-eq)	9.3 (ax-ax)	3.3 (ax-eq)
$^{3}J_{H4\text{-}H3}$	9.4 (ax-ax)	3.7 (ax-eq)	3.9 (ax-eq)
$^{3}J_{H3\text{-}H2ax}$	12.0 (ax-ax)	3.1 (ax-eq)	11.9 (ax-ax)
$^{3}J_{H3\text{-}H2eq}$	5.4 (ax-eq)	3.8 (eq-eq)	6.0 (ax-eq)
$^{4}J_{H6eq\text{-}H2eq}$	2.7 (eq-eq)	2.8 (eq-eq)	1.6 (eq-eq)
Coupling	QA6	QA7	QA8
$^{2}J_{H6ax\text{-}H6eq}$	− 14.3 (ax-eq)	− 14.0 (ax-eq)	− 14.3 (ax-eq)
$^{2}J_{H2ax\text{-}H2eq}$	− 14.5 (ax-eq)	− 15.5 (ax-eq)	− 13.7 (ax-eq)
$^{3}J_{H6ax\text{-}H5}$	11.8 (ax-ax)	11.3 (ax-ax)	11.4 (ax-ax)
$^{3}J_{H6eq\text{-}H5}$	5.6 (ax-eq)	5.7 (ax-eq)	5.8 (ax-eq)
$^{3}J_{H5\text{-}H4}$	9.3 (ax-ax)	3.1 (ax-eq)	9.3 (ax-ax)
$^{3}J_{H4\text{-}H3}$	9.0 (ax-ax)	3.5 (ax-eq)	9.1 (ax-ax)
$^{3}J_{H3\text{-}H2ax}$	11.9 (ax-ax)	12.5 (ax-ax)	11.8 (ax-ax)
$^{3}J_{H3\text{-}H2eq}$	5.6 (ax-eq)	5.7 (ax-eq)	5.5 (ax-eq)
$^{4}J_{H6eq\text{-}H2eq}$	2.6 (eq-eq)	2.1 (eq-eq)	2.1 (eq-eq)

Table 5 One bond ^{13}C-^{1}H coupling constants (in Hz) for all quinic acid isomers

$^{1}J_{C\text{-}H}$	QA1/QA3	QA2/QA4	QA5	QA6	QA7	QA8
$^{1}J_{C2\text{-}Hax}$	133.6 (ax)	134.4 (ax)	134.7 (ax)	132.9 (ax)	136.9 (ax)	132.6 (ax)
$^{1}J_{C2\text{-}Heq}$	138.3 (eq)	137.9 (eq)	139.8 (eq)	136.8 (eq)	135.9 (eq)	139.1 (eq)
$^{1}J_{C3\text{-}H}$	150.4 (ax)	158.2 (eq)	153.4 (ax)	149.7 (ax)	149.0 (ax)	151.2 (ax)
$^{1}J_{C4\text{-}H}$	148.8 (ax)	149.7 (ax)	155.2 (eq)	147.7 (ax)	155.1 (eq)	147.4 (ax)
$^{1}J_{C5\text{-}H}$	153.9 (eq)	147.9 (ax)	152.0 (ax)	149.5 (ax)	150.5 (ax)	152.3 (ax)
$^{1}J_{C6\text{-}Hax}$	132.4 (ax)	134.6 (ax)	134.5 (ax)	135.2 (ax)	135.9 (ax)	134.3 (ax)
$^{1}J_{C6\text{-}Heq}$	138.4 (eq)	137.8 (eq)	137.7 (eq)	137.1 (eq)	136.4 (eq)	139.0 (eq)

(axial or equatorial) of the coupling protons and/or the orientation of the hydroxy groups attached to the coupling carbon, as discussed below.

The one-bond ^{13}C-^{1}H coupling constants (Table 5) are mainly dependent upon the orientation of the proton. For the $J_{C2\text{-}H}$ and $J_{C6\text{-}H}$ coupling constants, the values are larger for couplings with equatorial than axial protons (axial: 132.4 – 136.2 Hz; equatorial: 136.4 – 139.5 Hz). This holds also true for the other couplings. The largest values within an isomer always occur for equatorial couplings, which range from 151.8 to 158.4 Hz. The axial couplings are slightly smaller, ranging from 147.4 to 152.3 Hz. For all conformers, the $J_{C3\text{-}H}$, $J_{C4\text{-}H}$, and $J_{C5\text{-}H}$ couplings are larger than the $J_{C2\text{-}H}$ and $J_{C6\text{-}H}$ couplings.

The $^{2}J_{CH}$ couplings (Table 6) are affected by both the orientation of the coupling proton and the hydroxy group on the coupling carbon. Couplings to axial protons are affected by the orientation of the hydroxy group attached to the coupling carbon atom. This is very clear for the $^{2}J_{C1\text{-}H2ax}$, $^{2}J_{C1\text{-}H6ax}$, $^{2}J_{C3\text{-}H2ax}$, and $^{2}J_{C5\text{-}H6ax}$ couplings; the couplings are small negative or slight positive (−1.9 – 0.5 Hz) when the hydroxy group is in the axial position and more negative (−5.1 to −6.5 Hz) otherwise. A similar effect can also be seen for the $^{2}J_{C3\text{-}H4}$, $^{2}J_{C4\text{-}H3}$, $^{2}J_{C4\text{-}H5}$ and $^{2}J_{C5H4}$ couplings, which are positive (1.8–2.6 Hz) when the both the coupling proton and the hydroxy attached to the carbon are axial, and negative (−2.5 to −4.4 Hz) otherwise. A similar effect is not observed for couplings to equatorial protons.

The three-bond ^{13}C-^{1}H couplings are presented in Table 7. These couplings mainly depend on the position of the coupling proton. Couplings of carbons with equatorial protons are larger (between 4.0 and 10.3 Hz) than those with axial protons (which range from 0.0 to 2.7 Hz). This correlates with the dihedral angle defined by the coupling atoms (listed in the Supporting Information): the couplings are generally large when the dihedral angle is close to 180° (equatorial couplings) and smaller for angles around 60 and −60° (axial couplings). The orientation of the hydroxy group attached to the coupling carbon affects some of the couplings: the $^{3}J_{C4\text{-}H2eq}$ and $^{3}J_{C4\text{-}H6eq}$ couplings are larger (in QA1–4, QA6, and QA8; 8.2 – 9.0 Hz) when the hydroxy group is in the equatorial position than when it is axial (in QA5 and QA7; 5.8 to 6.0 Hz).

Table 6 Two-bond ^{13}C-^{1}H coupling constants (in Hz) for all quinic acid isomers

$^{2}J_{C\text{-}H}$	QA1/QA3	QA2/QA4	QA5	QA6	QA7	QA8
$^{2}J_{C1\text{-}H2ax}$	− 5.1 (ax)	− 0.9 (ax)	− 6.3 (ax)	− 0.3 (ax)	− 1.9 (ax)	− 5.8 (ax)
$^{2}J_{C1\text{-}H2eq}$	− 5.7 (eq)	− 0.3 (eq)	− 4.3 (eq)	− 4.5 (eq)	− 4.3 (eq)	− 4.0 (eq)
$^{2}J_{C1\text{-}H6ax}$	− 5.7 (ax)	− 0.6 (ax)	− 5.7 (ax)	− 1.4 (ax)	0.0 (ax)	− 6.0 (ax)
$^{2}J_{C1\text{-}H6eq}$	− 4.1 (eq)	− 5.1 (eq)	− 4.0 (eq)	− 5.3 (eq)	− 5.0 (eq)	− 4.7 (eq)
$^{2}J_{C2\text{-}H3}$	0.0 (ax)	− 1.0 (eq)	− 1.6 (ax)	− 1.9 (ax)	− 1.4 (ax)	− 1.5 (ax)
$^{2}J_{C3\text{-}H4}$	− 3.3 (ax)	2.6 (ax)	− 2.8 (eq)	− 4.1 (ax)	− 3.3 (eq)	− 4.4 (ax)
$^{2}J_{C3\text{-}H2ax}$	− 5.9 (ax)	0.5 (ax)	− 6.4 (ax)	− 5.8 (ax)	− 6.1 (ax)	− 6.4 (ax)
$^{2}J_{C3\text{-}H2eq}$	− 4.8 (eq)	− 4.9 (eq)	− 3.8 (eq)	− 4.6 (eq)	− 3.5 (eq)	− 4.6 (eq)
$^{2}J_{C4\text{-}H3}$	− 4.4 (ax)	− 3.0 (eq)	1.8 (ax)	− 2.5 (ax)	1.8 (ax)	− 2.5 (ax)
$^{2}J_{C4\text{-}H5}$	− 3.0 (eq)	− 4.5 (ax)	2.3 (ax)	− 4.3 (ax)	2.6 (ax)	− 4.5 (ax)
$^{2}J_{C5\text{-}H4}$	2.2 (ax)	− 3.2 (ax)	− 1.7 (eq)	− 3.0 (ax)	− 2.2 (eq)	− 3.4 (ax)
$^{2}J_{C5\text{-}H6ax}$	− 0.2 (ax)	− 5.5 (ax)	− 6.5 (ax)	− 5.8 (ax)	− 5.8 (ax)	− 6.2 (ax)
$^{2}J_{C5\text{-}H6eq}$	− 5.2 (eq)	− 4.5 (eq)	− 3.6 (eq)	− 4.2 (eq)	− 3.5 (eq)	− 4.0 (eq)

Table 7 Three-bond ^{13}C-^{1}H coupling constants (in Hz) for all quinic acid isomers

$^{3}J_{C\text{-}H}$	QA1/QA3	QA2/QA4	QA5	QA6	QA7	QA8
$^{3}J_{C1\text{-}H3}$	0.3 (ax)	7.9 (eq)	0.7 (ax)	0.5 (ax)	0.4 (ax)	0.3 (ax)
$^{3}J_{C1\text{-}H5}$	8.6 (eq)	0.5 (ax)	0.6 (ax)	0.3 (ax)	0.3 (ax)	0.0 (ax)
$^{3}J_{C2\text{-}H6ax}$	1.6 (ax)	0.9 (ax)	0.9 (ax)	0.8 (ax)	0.9 (ax)	1.9 (ax)
$^{3}J_{C2\text{-}H6eq}$	6.4 (eq)	6.5 (eq)	5.8 (eq)	6.4 (eq)	5.5 (eq)	7.0 (eq)
$^{3}J_{C2\text{-}H4}$	1.3 (ax)	0.4 (ax)	4.1 (eq)	1.6 (ax)	4.2 (eq)	1.8 (ax)
$^{3}J_{C3\text{-}H5}$	6.4 (eq)	1.0 (ax)	0.4 (ax)	1.5 (ax)	0.5 (ax)	1.3 (ax)
$^{3}J_{C4\text{-}H2ax}$	2.7 (ax)	1.0 (ax)	1.8 (ax)	2.7 (ax)	1.7 (ax)	3.1 (ax)
$^{3}J_{C4\text{-}H2eq}$	8.4 (eq)	8.7 (eq)	6.2 (eq)	9.0 (eq)	5.8 (eq)	9.0 (eq)
$^{3}J_{C4\text{-}H6ax}$	1.2 (ax)	2.3 (ax)	1.8 (ax)	2.5 (ax)	1.8 (ax)	2.5 (ax)
$^{3}J_{C4\text{-}H6eq}$	9.0 (eq)	8.3 (eq)	5.8 (eq)	8.9 (eq)	6.0 (eq)	8.9 (eq)
$^{3}J_{C5\text{-}H3}$	1.1 (ax)	5.5 (eq)	0.3 (ax)	1.1 (ax)	0.4 (ax)	0.9 (ax)
$^{3}J_{C6\text{-}H4}$	0.4 (ax)	1.1 (ax)	4.2 (eq)	1.4 (ax)	4.1 (eq)	1.4 (ax)

^{1}H and ^{13}C-NMR chemical shifts for the quinic acid isomers

Tables 8 and 9 show the computed ^{1}H and ^{13}C NMR chemical shifts, respectively. The ^{1}H chemical shifts are larger (3.5 to 4.5 ppm) for protons bound to C3, C4, and C5, compared to C2 and C6. This is caused by the deshielding effect of the electron-withdrawing hydroxy substituents on these carbons.

The ^{13}C chemical shifts in general are within a broad range and can have values from as small as −10 to > 200 ppm. For quinic acid, the values roughly fall into three different categories: the smallest ones (around 45 ppm) occur for C2 and C6, which do not have electron-withdrawing groups attached; the values are around 75–80 ppm for C3, C4, and C5, due to the deshielding effect of the hydroxy groups attached to these carbons; the most downfield ^{13}C chemical shifts are for the carboxylic acid carbon, with values between 181 and 186 ppm, which are typical for carboxylic acid carbons.

Table 8 ^{1}H-NMR chemical shifts (in ppm)

^{1}H	QA1/QA3	QA2/QA4	QA5	QA6	QA7	QA8
H2ax	1.5	1.9	1.8	1.7	2.4	1.5
H2eq	2.4	2.1	2.1	2.1	1.7	2.3
H3	4.3	4.5	4.2	4.1	3.8	4.0
H4	3.6	3.7	4.3	3.5	4.3	3.5
H5	4.2	4.2	4.1	3.9	4.2	4.3
H6ax	1.8	1.9	1.8	2.0	1.9	1.6
H6eq	2.6	2.0	1.9	2.0	1.7	2.2

Referenced to TMS. The TMS ^{1}H chemical shielding is 31.994 ppm

Table 9 ^{13}C-NMR chemical shifts (in ppm)

^{13}C	QA1/QA3	QA2/QA4	QA5	QA6	QA7	QA8
C1	79.9	84.1	81.1	82.3	83.9	81.0
C2	44.7	40.5	44.6	46.6	41.0	46.6
C3	75.7	77.2	74.1	75.5	73.4	74.5
C4	81.5	80.7	77.3	85.9	77.8	85.8
C5	74.3	75.4	74.6	77.1	74.7	77.2
C6	46.3	45.9	43.9	44.6	40.5	48.7
C(OOH)	180.8	181.9	182.2	182.2	181.9	182.2

Referenced to TMS. The TMS ^{13}C chemical shielding is 185.01 ppm

Conclusions

We calculated geometries, NMR spin-spin coupling constants, and chemical shifts of the eight stereoisomers of quinic acid. Both levels of theory applied in this study, B3LYP/6-311G(d,p) (mixed), and B3LYP/EPR-II (mixed), both in methanol continuum solvent, produced reliable geometries and NMR parameters. The calculated coupling constants were found to be the key determinants for differentiation and identification of the different stereoisomers: The magnitude of the $^{3}J_{HH}$ couplings depends on the position (axial or equatorial) of the coupling protons, whereas the ^{13}C-^{1}H couplings primarily depend on the orientation of the coupling proton and/or the orientation of the hydroxy groups attached to the coupling carbon. Thus, the computational data provided here can be used to provide reliable assignments of the positions of the hydroxy groups for quinic acids isolated from plants or for synthesized quinic acid derivatives. Analogous DFT techniques can be used to differentiate between different stereoisomers of systems similar to quinic acid, such as octulosonic acid.

Acknowledgements We are grateful to EaStCHEM for computational support via the EaStCHEM Research Computing Facility. RH acknowledges funding from the Higher Education Commission of Pakistan for her visit to University of St-Andrews, as a visiting scholar. AK is thankful to the Higher Education Commission of Pakistan (Grant No. 1691) as well as to the COMSATS University Islamabad, Abbottabad Campus for financial support.

References

1. Albertini E, Barco A, Benetti S, De Risi C, Pollini GP, Zanirato V (1997) Enantioselective approach to 7-azabicyclo[2.2.1]heptane ring systems using D-(−)-quinic acid as the chiral educt: application to the formal synthesis of (+)-epibatidine. Tetrahedron Lett 38:681–684
2. Barco A, Benetti S, Risi CD, Marchetti P, Pollini GP, Zanirato V (1997) D-(−)-Quinic acid: a chiron store for natural product synthesis. Tetrahedron Asymmetry 8:3515–3545
3. Deshpande S, Matei MF, Jaiswal R, Bassil BS, Kortz U, Kuhnert N (2016) Synthesis, structure, and tandem mass spectrometric characterization of the diastereomers of quinic acid. J Agrid Food Chem 64:7298–7306
4. Pauli GF, Poetsch F, Nahrstedt A (1998) Structure assignment of natural quinic acid derivatives using proton nuclear magnetic resonance techniques. Phytochem Anal 9:177–185
5. Anet EFLJ, Reynolds TM (1953) Isolation of l-quinic acid from the peach fruit. Nature 172:1188–1189
6. Nishizawa M, Yamagishi T, Dutschman GE, Parker WB, Bodner AJ, Kilkuskie RE, Cheng Y-C, Lee K-H (1989) Anti-AIDS agents, 1. Isolation and characterization of four new tetragalloylquinic acids as a new class of HIV reverse transcriptase inhibitors from tannic acid. J Nat Prod 52:762–768
7. Merfort I (1992) Caffeoylquinic acids from flowers of *Arnica montana* and *Arnica chamissonis*. Phytochemistry 31:2111–2113
8. Baratto MC, Tattini M, Galardi C, Pinelli P, Romani A, Visioli F, Basosi R, Pogni R (2003) Antioxidant activity of galloyl quinic derivatives isolated from *P. lentiscus* leaves. Free Radic Res 37:405–412
9. Hung TM, Na M, Thuong PT, Su ND, Sok D, Song KS, Seong YH, Bae K (2006) Antioxidant activity of caffeoyl quinic acid derivatives from the roots of *Dipsacus asper* Wall. J Ethnopharmacol 108:188–192
10. Kim KH, Kim YH, Lee KR (2007) Isolation of quinic acid derivatives and flavonoids from the aerial parts of *Lactuca indica* L. and their hepatoprotective activity in vitro. Bioorg Med Chem Lett 17:6739–6743
11. Basnet P, Matsushige K, Hase K, Kadota S, Namba T (1996) Potent antihepatotoxic activity of dicaffeoyl quinic acids from propolis. Biol Pharm Bull 19:655–657
12. Hur JY, Soh Y, Kim B-H, Suk K, Sohn NW, Kim HC, Kwon HC, Lee KR, Kim SY (2001) Neuroprotective and neurotrophic effects of quinic acids from *Aster scaber* in PC12 cells. Biol Pharm Bull 24:921–924
13. Abrankó L, Clifford MN (2017) An unambiguous nomenclature for the acyl-quinic acids commonly known as chlorogenic acids. J Agrid Food Chem 65:3602–3608
14. Scholz-Böttcher BM, Ernst L, Maier HG (1991) New stereoisomers of quinic acid and their lactones. Liebigs Ann Chem 1991:1029–1036
15. Corse J, Lundin RE (1970) Diastereomers of quinic acid. Chemical and nuclear magnetic resonance studies. J Organomet Chem 35:1904–1909
16. Härtner J, Reinscheid UM (2008) Conformational analysis of menthol diastereomers by NMR and DFT computation. J Mol Struct 872:145–149
17. Frisch MJ, Trucks GW, Schlegel HB, Scuseria GE, Robb MA, Cheeseman JR, Scalmani G, Barone V, Mennucci B, Petersson GA, Nakatsuji H, Caricato M, Li X, Hratchian HP, Izmaylov AF, Bloino J, Zheng G, Sonnenberg JL, Hada M, Ehara M, Toyota K, Fukuda R, Hasegawa J, Ishida M, Nakajima T, Honda Y, Kitao O, Nakai H, Vreven T, Montgomery JA, Peralta JE, Ogliaro F, Bearpark M, Heyd JJ, Brothers E, Kudin KN, Staroverov VN, Kobayashi R, Normand J, Raghavachari K, Rendell A, Burant JC, Iyengar SS, Tomasi J, Cossi M, Rega N, Millam JM, Klene M, Knox JE, Cross JB, Bakken V, Adamo C, Jaramillo J, Gomperts R, Stratmann RE, Yazyev O, Austin AJ, Cammi R, Pomelli C, Ochterski JW, Martin RL, Morokuma K, Zakrzewski VG, Voth GA, Salvador P, Dannenberg JJ, Dapprich S, Daniels AD, Farkas Ö, Foresman JB, Ortiz JV, Cioslowski J, Fox DJ (2009) Gaussian, Inc., Wallingford
18. Becke AD (1988) Density-functional exchange-energy approximation with correct asymptotic behavior. Phys Rev A 38:3098–3100
19. Becke AD (1993) Density functional thermochemistry. 3. The role of exact exchange. J Chem Phys 98:5648–5652
20. Lee C, Yang W, Parr RG (1988). Phys Rev B 37:785–789
21. Krishnan, R, Binkley, JS, Seeger, R, Pople, JA (1980) Self-consistent molecular orbital methods. XX. A basis set for correlated wave functions. J Chem Phys 72:650–654
22. Miertus S, Scrocco E, Tomasi J (1981) Electrostatic interaction of a solute with a continuum. A direct utilization of ab initio molecular potentials for the prevision of solvent effects. Chem Phys 55:117–129
23. Mennucci B (1998) Excited states and solvatochromic shifts within a nonequilibrium solvation approach: a new formulation of the integral equation formalism method at the self-consistent field, configuration interaction, and multiconfiguration self-consistent field level. J Chem Phys 109:2798–2807
24. Ding Y, Su Y, Guo H, Yang F, Mao H, Gao X, Zhu Z, Tu G (2010) Phenylpropanoyl esters from horseweed (*Conyza canadensis*) and their inhibitory effects on catecholamine secretion. J Nat Prod 73:270–274
25. Barone V (1996) In recent advances in density functional methods, Part I. In: Chong DP (ed) World Scientific Publ. Co., Singapore
26. Cheeseman JR, Trucks GW, Todd AK, Frisch MJ (1996) A comparison of models for calculating nuclear magnetic resonance shielding tensors. J Chem Phys 104:5497–5509
27. Ditchfield R (1974). Mol Phys 27:789–807
28. Wolinsky K, Hilton JF, Pulay P (1990) Efficient implementation of the gauge-independent atomic orbital method for NMR chemical shift calculations. J Am Chem Soc 112:8251–8260
29. Ramsay NF (1953) Electron coupled interactions between nuclear spins in molecules. Phys Rev 91:303–307
30. Takenaka M, Ono H (2003) Novel octulosonic acid derivatives in the composite *Smallanthus sonchifolius*. Tetrahedron Lett 44:999–1002